Developmental Biology 369 (2012) 340–348

Contents lists available at SciVerse ScienceDirect

Developmental Biology

journal homepage: www.elsevier.com/locate/developmentalbiology

FGF9–Pitx2–FGF10 signaling controls cecal formation in mice

Denise Al Alam [a], Frederic G. Sala [a], Sheryl Baptista [a], Rosanna Galzote [a], Soula Danopoulos [a], Caterina Tiozzo [a], Philip Gage [b], Tracy Grikscheit [a], David Warburton [a], Mark R. Frey [a], Saverio Bellusci [a,c,*]

[a] Developmental Biology and Regenerative Medicine Program, Saban Research Institute of Children's Hospital Los Angeles, Los Angeles, CA 90027, USA
[b] University of Michigan Kellogg Eye Center, 1000 Wall Street, Ann Arbor, MI, USA
[c] Excellence Cluster in Cardio-Pulmonary Systems, Department of Internal Medicine II, University of Giessen Lung Center, Klinikstrasse 36, 35392 Giessen, Germany

ARTICLE INFO

Article history:
Received 22 December 2011
Received in revised form
19 June 2012
Accepted 10 July 2012
Available online 20 July 2012

Keywords:
Pitx2
Fgf9
Fgf10
Cecum
Agenesis
Development

ABSTRACT

Fibroblast growth factor (FGF) signaling to the epithelium and mesenchyme mediated by FGF10 and FGF9, respectively, controls cecal formation during embryonic development. In particular, mesenchymal FGF10 signals to the epithelium via FGFR2b to induce epithelial cecal progenitor cell proliferation. Yet the precise upstream mechanisms controlling mesenchymal FGF10 signaling are unknown. Complete deletion of *Fgf9* as well as of *Pitx2*, a gene encoding a homeobox transcription factor, both lead to cecal agenesis. Herein, we used mouse genetic approaches to determine the precise contribution of the epithelium and/or mesenchyme tissue compartments in this process. Using tissue compartment specific *Fgf9* versus *Pitx2* loss of function approaches in the gut epithelium and/or mesenchyme, we determined that FGF9 signals to the mesenchyme via *Pitx2* to induce mesenchymal *Fgf10* expression, which in turn leads to epithelial cecal bud formation.

Introduction

The cecum forms a pouch contiguous with the gastrointestinal (GI) tract, lying between the ileum and the large intestine or colon. Hosting a large reservoir of microbes, the cecum plays an important role in the digestion of small food particles and complex carbohydrates from plant matter. Thus, this part of the gut tends to be more prominent in herbivores and omnivores than obligate carnivores (Backhed et al., 2005; Eckburg et al., 2005). In mouse embryogenesis, the cecum starts to form at E10.5 as a mesenchymal expansion, followed by an epithelial evagination (Burns et al., 2004). Epithelial evagination initiation is then followed by elongation (growth), differentiation and arrest. To date, however, the signals defining cecal development remain incompletely understood.

The cecum, like other parts of the intestine, is composed of two layers: an endoderm-derived epithelium and the surrounding mesoderm-derived mesenchyme. Epithelial–mesenchymal interactions are required for proper budding morphogenesis and differentiation in many organs including the gut (Cardoso, 2001; Koike and Yasugi, 1999; Shannon and Hyatt, 2004). Fibroblast growth factors, key elements of epithelial–mesenchymal interactions in many tissues, have been described as major players in controlling cecum formation. We have shown that loss of FGFR2b signaling, in *Fgf10* or *Fgfr2IIIb* knock-out (K.O.) embryos, results in the formation of a mesenchymal expansion, but the epithelium fails to proliferate and bud (Burns et al., 2004; Fairbanks et al., 2004). Moreover, the guts of *Fgf9* null embryos display complete cecal agenesis, with the absence of both mesenchymal expansion and epithelial budding. This is accompanied with decreased mesenchymal proliferation as well as complete lack of *Bmp4* and *Fgf10* expression. In turn, absence of *Fgf10* resulted in decreased epithelial proliferation (Zhang et al., 2006). During embryonic development, *Fgf9* is mostly found in the epithelium of the cecum but is also detected at lower levels in the mesenchyme. However, compartment specific (epithelial vs. mesenchymal) deletion of *Fgf9* in the cecum has not yet been studied.

Pitx2 is a member of the homeobox gene family that encodes a transcription factor initially identified as a gene mutated in Axenfeld–Rieger Syndrome type I, a rare autosomal dominant disorder that affects the development of the teeth, eyes and umbilicus (Semina et al., 1996a). In the GI tract, *Pitx2* is mainly expressed in the mesenchyme of the developing cecum (Burns et al., 2004) and it was recently reported that classical *Pitx2* inactivation in mouse leads to cecal agenesis (Nichol and Saijoh, 2011). In addition, it has been shown that over-expression of *Hoxd12*, another homeobox gene, phenocopies the loss of *Fgf9* and

* Corresponding author at: Developmental Biology and Regenerative Medicine Program, Saban Research Institute of Children's Hospital Los Angeles, 4650 W Sunset Boulevard, MS#35, Los Angeles, CA 90027, USA.
E-mail address: sbellusci@chla.usc.edu (S. Bellusci).

0012-1606/$ - see front matter © 2012 Elsevier Inc. All rights reserved.
http://dx.doi.org/10.1016/j.ydbio.2012.07.008

leads to cecal agenesis and loss of *Fgf10* and *Pitx1* expression (Zacchetti et al., 2007).

Developmental studies of branching processes in different organs, e.g. cecum and lung, suggest that the mechanisms controlling branching are substantially conserved between organs. We have reported previously that deletion of mesenchymal *β-catenin* in the embryonic lung results in a loss of *Pitx2* and *Fgf10* expression. This was associated with impaired epithelial and mesothelial FGF9 signaling to the mesenchyme due to decreased expression of *Fgfr2-IIIc* (De Langhe et al., 2008). These results led us to propose that an FGF9/Pitx2/FGF10 signaling pathway controls lung bud formation. In the current study, we have used tissue specific *Fgf9* and *Pitx2* loss of function approaches in the gut epithelium and mesenchyme to show that this signaling axis is active in the developing gut, and demonstrate its importance for cecal formation.

Materials and methods

Transgenic embryos

Dermo1-Cre (C57Bl/6 background), and $Fgf9^{flox/flox}$ mice were obtained from Dr. David Ornitz (Washington University, Saint Louis, MO (Yu et al., 2003)) and Dr. Fen Wang (Institute of Biosciences and Technology, Houston, TX (Lin et al., 2006)) respectively. $Pitx2^{flox/flox}$ mice were previously described (Gage et al., 1999). *Dermo1-Cre* mice were crossed with $Pitx2^{flox/flox}$ mice to generate [*Dermo1-Cre*; $Pitx2^{flox/+}$] that were then crossed with $Pitx2^{flox/flox}$ mice to generate [*Dermo1-Cre*; $Pitx2^{flox/flox}$] mutant embryos (called hereafter $Pitx2^{Dermo1\text{-}Cre}$). *Shh-Cre* mice were purchased from The Jackson Laboratory and were used to inactivate *Pitx2* specifically in the epithelium. *Shh-Cre* mice were crossed with $Pitx2^{flox/flox}$ mice to generate [*Shh-Cre*, $Pitx2^{f/+}$] that were then crossed with $Pitx2^{flox/flox}$ mice to generate [*Shh-Cre;* $Pitx2^{flox/flox}$] mutant embryos (called hereafter $Pitx2^{Shh\text{-}Cre}$). To inactivate *Fgf9* in the mesenchyme, we used *Dermo1-Cre* as described above for *Pitx2* inactivation. *CMV-Cre* mice were also used to completely inactivate *Fgf9* throughout the embryo including both epithelium and mesenchyme of the gut. Animal experiments were performed under the research protocol (31-08) approved by the Animal Research Committee at Children's Hospital Los Angeles and in strict accordance with the recommendations in the Guide for the Care and Use of Laboratory Animals of the National Institutes of Health. The approval identification for Children's Hospital Los Angeles is AAALAC A3276-01.

Whole mount in situ hybridization (WISH)

Microdissected guts were fixed in 4% paraformaldehyde (PFA) for 20 min and dehydrated in ethanol. The samples were washed twice in PBS for 10 min, transferred and stored in 70% ethanol until use. Whole-mount in situ hybridization protocol was performed as described (Winnier et al., 1995). The following mouse cDNAs were used as templates for the synthesis of digoxigenin-labeled riboprobes: a 528 bp fragment of *Fgf9* (provided by Dr. Ornitz), a 642 bp fragment of *Shh* (a kind gift from Dr Andrew McMahon, Harvard University, Boston, MA), a 584 bp fragment of *Fgf10* (Bellusci et al., 1997), a 1.5 kb full-length mouse *Bmp4* (Winnier et al., 1995), and a 559 bp fragment of *Pitx2* present in all 3 *Pitx2* isoforms (De Langhe et al., 2008). Sense probes were used for negative controls on E12.5 wild type ceca.

Proliferation analysis

Intraperitoneal injection of 0.2 mL bromodeoxyuridine (BrdU, Amersham Biosciences UK) was given to pregnant females (4 pregnant females) carrying mutant and littermate control embryos at E12.5. The females were sacrificed 15 min later and the embryos were immediately placed in ice-cold Hank's solution. The ceca were dissected from the embryos, fixed in 4% PFA, gradually dehydrated in ethanol and processed for paraffin sectioning. The ceca ($n=6$) were uniformly dissected and oriented away from the label of the embedding cassette or slide, with a short segment of the Ileum and a segment of the colon towards label. The embedded specimens were sectioned at 5 μm. The sections were re-hydrated and the antigen was retrieved by boiling the slides for 15 min in a microwave in 10 mM sodium citrate (pH 6.0). The slides were incubated for 1 h with monoclonal anti-BrdU antibody (Clone BU-1) RPN 202 as recommended by the manufacturer (Amersham Biosciences, UK). Cy3-labeled anti-mouse secondary antibodies were used. The slides were then mounted using Vectashield containing DAPI and photographed. The epithelial and mesenchymal cells of the cecum were counted separately for the number of total cells and BrdU-labeled cells. The boundaries of the mutant ceca were defined by the mesenchymal thickness and the curvature angles on each side, as illustrated in Fig. 4, panel K. The results are reported as the percentage of BrdU-positive cells. Tissues from females not injected with BrdU, and sections stained with secondary antibody alone were used as negative controls. No staining was observed in these specimens.

Quantitative PCR analyses

RNA was extracted from individually microdissected ceca from $Pitx2^{Dermo1\text{-}Cre}$ mutant and littermate control embryos at E12.5 ($n=8$). One microgram of RNA was reverse-transcribed into cDNA using Transcriptor High Fidelity cDNA Synthesis Kit (Roche Applied Science, Indianapolis, USA) according to the manufacturer's instructions. cDNA (2 μL) was used for dual color Hydrolysis Probe—Universal probe library based real time PCR, using the LightCycler 480 from Roche Applied Science. Mouse GAPDH gene assay (Roche applied Science) was used as the reference gene. The sets of primers and probe used for each gene examined are *Bmp4* (Forward: GAGGAGTTTCCATCACGAAGA, Reverse: GCTCTGCCGAGGAGATCA, Probe 89), *Fgf9* (Forward: GGGGAGCTGTATGGATCAGA, Reverse: TCCCGTCCTTATTTAATGCAA, Probe 12), *Fgf10* (Forward: CGGGACCAAGAATGAAGACT, Reverse: AACAACTCCAGATTTCCACTGA, Probe 80), *Pitx2* (Forward: CCTTACGGAAGCCCGAGT, Reverse: CCAAGCCATTCTTGCACA, Probe 40), *Fgfr2b* (Forward: CCCTACCTCAAGGTCCTGAA, Reverse: CATCCATCTCCGTCACATTG, Probe 21), *Fgfr2c* (Forward: TGCATGGTTGACAGTTCTGC, Reverse: TGCAGGCGATTAAGAAGACC, Probe 60). mRNA and water were used as negative controls.

In vitro cecum culture

Ceca were microdissected from wild type C57Bl/6 mice at E12.5, and placed atop polycarbonate filters (13 mm diameter, 8 μm pore size, Whatman) in 1 mL DMEM/F12 supplemented with 5% Fetal Bovine Serum and 1% Penicillin/Streptomycin. Ceca were then incubated with or without 250 ng/mL of human recombinant FGF9 ($n=4$ in duplicates) at 37 °C for 12 h in a moist atmosphere (5% CO_2).

Ectopic Pitx2 expression in cultured fibroblasts

NIH 3T3 murine fibroblasts (ATCC, #CRL-1658) were grown in DMEM with 10% FBS to 80% confluence. Cultures were transfected with plasmid encoding human *Pitx2* (pCI-HA*Pitx2a*) (Kozlowski and Walter, 2000) or empty vector (pCI) in Opti-MEM (Gibco Life Technologies) using Lipofectamine 2000 (Invitrogen), following the manufacturer's recommended protocol. Forty-eight hours

after transfection, cellular RNA was isolated for qRT-PCR analysis of *Pitx2*, *Fgf9*, and *Fgf10* expression.

Statistical analyses

Statistical analyses were performed using Graphpad Prism software. All data are expressed as mean ± SEM. Comparisons of the changes between controls and DTG were performed using paired wilcoxon test. A $p \leq 0.05$ was considered significant. The proliferation and quantitative PCR analyses were performed on mutants and control littermates from at least 4 pregnant females. Each litter carried 1–3 mutants and several controls. The statistical analyses were performed on paired samples; in each experiment, *n* designates the number of embryos.

Results

Pitx2 expression in the developing mouse cecum

Previous studies have shown that *Pitx2* is expressed in several organs including the left lateral plate mesoderm, eye, brain, pituitary glands, mandible, heart, lung, limbs and teeth (Arakawa et al., 1998; De Langhe et al., 2008; Gage and Camper, 1997; Green et al., 2001; Kitamura et al., 1997; Muccielli et al., 1996; Semina et al., 1996b). It is also expressed in the developing mouse gut at E12.5, the midgut at E16.5, and in the cecum at E10.5 and E11.5 (Burns et al., 2004; Campione et al., 1999; Hjalt et al., 2000). However, the specific cellular compartments expressing *Pitx2* have not been clearly defined. To examine the spatial expression of *Pitx2* in the developing GI tract, we carried out whole mount in situ hybridization (WISH) for *Pitx2* on whole isolated GI tracts between E12.5 and E14.5. At these stages, *Pitx2* was strongly expressed in the small intestine and in the cecum, but absent in the colon as shown in Fig. 1A–C. Vibratome sections of the WISH samples showed that *Pitx2* is expressed in both epithelium and mesenchyme of the cecum at all the developmental stages studied (Fig. 1D–F). Interestingly, mesenchymal *Pitx2* expression is stronger at the apex of the bud compared to the stalk suggesting that it is directly involved in the proximal–distal growth of the cecal tube. However, in the small intestine *Pitx2* expression is restricted to the epithelium early on at E12.5 (Fig. 1G), while at E14.5, it is expressed in both epithelium and mesenchyme (Fig. 1H).

Specific deletion of Pitx2 in the mesenchyme results in cecal agenesis

It was recently reported that complete inactivation of *Pitx2* results in cecal agenesis (Nichol and Saijoh, 2011). Since *Pitx2* is expressed in both epithelium and mesenchyme of the cecum as shown in Fig. 1, it is unclear whether it is mesenchymal and/or epithelial *Pitx2* which is/are required for cecal budding and elongation. We therefore examined the development of the cecum in mice with *Pitx2* specifically deleted from the mesenchyme. Using the *Dermo1-Cre* driver line, *Pitx2* deletion in the mesenchyme resulted in embryonic lethality around E17.5 (data not shown). Therefore control and $Pitx2^{Dermo1\text{-}Cre}$ embryos at E11.5, E12.5, E14.5 and E16.5 were used for this study. We first

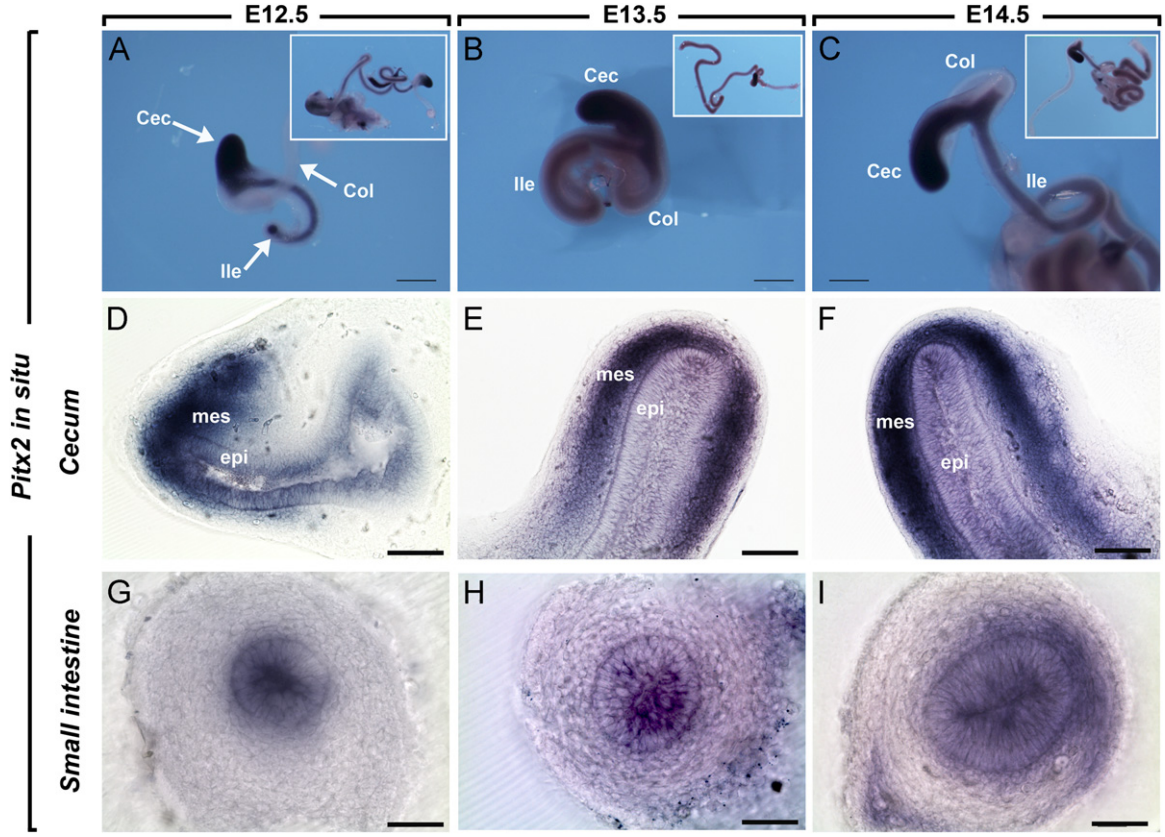

Fig. 1. *Pitx2* expression in the embryonic cecum. (A)–(C) Whole mount in situ hybridization was performed on isolated E12.5 (A), E13.5 (B) and E14.5 (C) GI tracts to detect *Pitx2* expression. *Pitx2* was strongly expressed in both epithelium and mesenchyme of the cecum, while *Pitx2* expression was restricted to the epithelium of the small intestine and absent in the colon. (D)–(F) Vibratome sections of the ceca were performed at 20 μm to show the localization of *Pitx2* at E12.5 (D), E13.5 (E) and E14.5 (F). The sections showed expression of *Pitx2* in both epithelium and mesenchyme of the cecum. (G) and (H) Vibratome sections of the small intestine to show the localization of *Pitx2* at E12.5 (G) and E14.5 (H). The sections showed an epithelial expression of *Pitx2* at E12.5 (G) and both mesenchymal and epithelial expression at E14.5 (H). Ile, ileum; Col, colon; cec, cecum; epi, epithelium; and mes, mesenchyme. Scale bars in (A)–(C) are 500 μm, scale bars in (D)–(I) are 100 μm.

confirmed specific *Pitx2* deletion in the mesenchyme of *Pitx2*$^{Dermo1\text{-}Cre}$ but not control (littermate *Dermo1-Cre*; *Pitx2*$^{fl/+}$) ceca at E11.5 (Fig. 2A and B). Note that *Pitx2* expression in the epithelium of the mutant gut was still maintained. *Dermo1-Cre*; *Pitx2*$^{fl/+}$ animals were morphologically similar to their control littermates at all stages (>70 embryos were analyzed for each genotype at each time point). At E12.5, the control cecum normally developed into a mesenchymal protrusion surrounding a layer of epithelial bud (Fig. 2C). In E12.5 *Pitx2*$^{Dermo1\text{-}Cre}$ mutants, both the mesenchymal protrusion and epithelial buds were absent ($n=70/70$ embryos examined) even though the characteristic bending of the gut at that location was still visible (Fig. 2D). At E14.5 the wild type cecum continued to develop (Fig. 2E) while the mutant cecum did not show any evidence of budding or elongation (Fig. 2F). A similar observation was made at E16.5 (Fig. 2G and H). In contrast to mesenchymal deletion, removing *Pitx2* from the epithelium using the *Shh*-Cre driver line did not affect cecal formation (Fig. 2I and J). Thus, we conclude that mesenchymal *Pitx2* but not epithelial *Pitx2* is required for cecal bud formation. Interestingly, we also observed that the small intestines of *Pitx2*$^{Dermo1\text{-}Cre}$ embryos are shorter than those of control littermates (Fig. 2L; 78.6% of the length of the controls at E14.5, $p=0.0125$, $n=7$, white arrows indicate the location of the cecum), whereas the colon lengths were similar (Fig. 2M). Additionally, around 65% of the mutants developed Meckel's diverticulum (black arrow, Fig. 2L) on the small intestine.

Decreased epithelial and mesenchymal cell proliferation after mesenchymal deletion of Pitx2

At E12.5, the epithelial and mesenchymal buds were normal in control embryos (Fig. 3A), whereas no epithelial or mesenchymal buds were observed in the mutant as shown by H&E staining (Fig. 3B). Since both mesenchymal and epithelial budding was affected in the mutant cecum, we assessed cell proliferation in these compartments using BrdU incorporation. Both epithelial and mesenchymal proliferations were reduced in the *Pitx2*$^{Dermo1\text{-}Cre}$ cecum (Fig. 3D and F) as compared to controls (Fig. 3C and E). Proliferation was reduced from 36.9% to 23.1% in the mesenchyme (Fig. 3G) ($p=0.05$, $n=6$) and from 45.2% to 27.4% in the epithelial cells ($p=0.05$, $n=6$) (Fig. 3G).

Fgf10 and Fgfr2b are down-regulated in the Pitx2$^{Dermo1\text{-}Cre}$ *cecum*

Loss of either *Fgf9* or *Fgf10* reduces proliferation in the epithelium and mesenchyme of the cecum (Burns et al., 2004; Zhang et al., 2006). Furthermore, the abnormalities we observed in the *Pitx2*$^{Dermo1\text{-}Cre}$ mutant cecum phenocopy those reported in *Fgf9* mutants. Therefore, we examined the expression of *Fgf9*, *Fgf10* and *Bmp4* in *Pitx2*$^{Dermo1\text{-}Cre}$ and control littermates using WISH and RT-qPCR. *Fgf10* was expressed in the mesenchyme of the cecum at E12.5 (Fig. 4A). However, in *Pitx2*$^{Dermo1\text{-}Cre}$ embryos, it was absent from the cecal mesenchyme as shown by WISH (Fig. 4B). *Bmp4* was expressed exclusively in the mesenchyme of the wild type cecum at E12.5 (Fig. 4C) and this expression was maintained in the *Pitx2*$^{Dermo1\text{-}Cre}$ mutant embryos (Fig. 4D). In contrast to *Bmp4*, *Fgf9* was expressed in both epithelium and mesenchyme of control cecum at E12.5 (Fig. 4E), whereas in *Pitx2*$^{Dermo1\text{-}Cre}$ animals it was only expressed in the epithelium (Fig. 4F, compare insets in E and F). WISH using sense probes for *Fgf10*, *Bmp4* and *Fgf9* on E12.5 wild-type ceca did not show any staining (Fig. 4G–I respectively).

The WISH data results were confirmed by qRT-PCR. The results showed a significant decrease in *Pitx2*, *Fgf10* and *Fgf9* levels in the mutant ceca as compared to controls ($p=0.024$, $p=0.025$ and $p=0.05$ respectively; Fig. 4J). No significant changes were detected in expression of *Bmp4* or *Fgfr2c*. Moreover, we found a statistically significant reduction in *Fgfr2b* ($p=0.023$) in the *Pitx2*

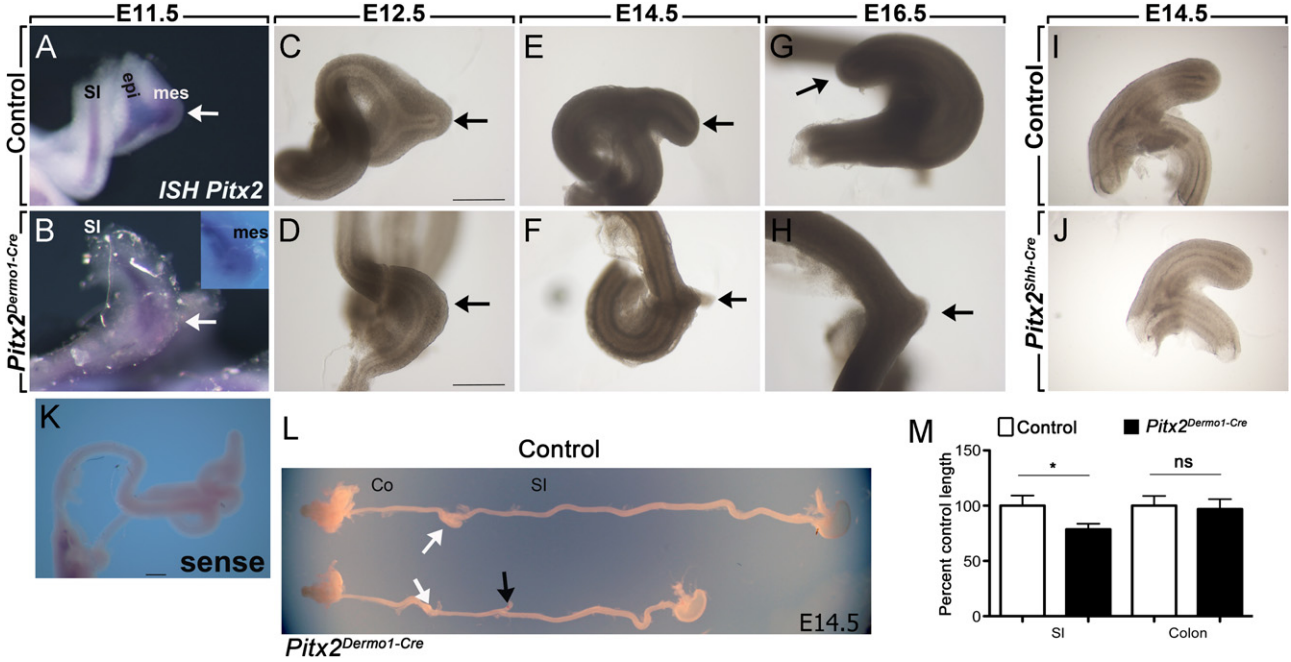

Fig. 2. Deletion of mesenchymal *Pitx2* leads to cecal agenesis. (A) *Pitx2* whole mount in situ hybridization (WMISH) confirms the deletion of mesenchymal *Pitx2* in the mutants (B) as compared to the controls at E11.5 (A). Comparison of the cecum development in E12.5 (C) and (D), E14.5 (E) and (F), and E16.5 (G) and (H) WT gut (C), (E), and (G) and *Pitx2*$^{Dermo1\text{-}Cre}$ gut (D), (F), and (H). *Pitx2*$^{Dermo1\text{-}Cre}$ mutants did not show any cecum formation (D), (F), and (H) whereas wild type littermates showed a normal developing cecum (C), (E), and (G). (I) and (J) Comparison of control (I) versus *Pitx2*$^{Shh\text{-}Cre}$ (J) ceca at E14.5. No difference is noticeable in the development of the mutant cecum compared to the control. (K) WISH using sense probe for Pitx2 did not show any staining in E12.5 wild type cecum. (L) Whole mount view of representative E14.5 GI tracts of *Pitx2*$^{Dermo1\text{-}Cre}$ and littermate controls. White arrows show the location of the cecum on each GI tract. The black arrow shows the diverticulum (M) quantification of the small intestine (SI) and colon lengths of *Pitx2*$^{Dermo1\text{-}Cre}$ mutants normalized to control littermates (100%) indicate that mutant SI are shorter when compared to controls while no difference is observed for the colons. The bars represent means $\pm$ s.e.m. Asterisk indicates a statistical difference ($p=0.0214$; $n=7$). Scale bars are 500 μm.

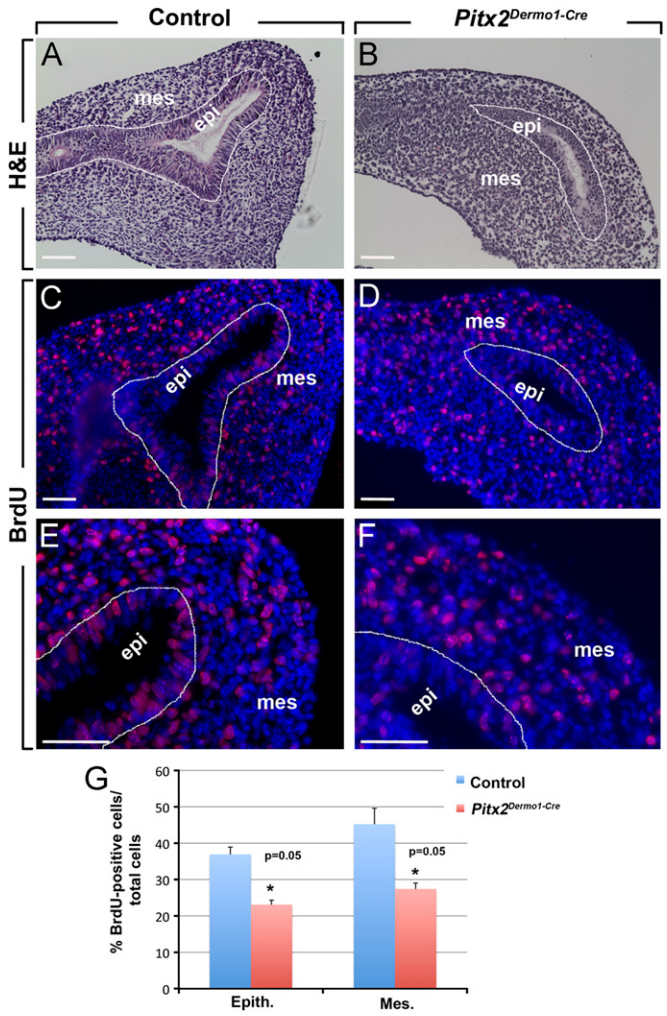

Fig. 3. Decrease in cell proliferation in *Pitx2*$^{Dermo1\text{-}Cre}$ mutants. (A) and (B) Paraffin sections from E12.5 control (A) and *Pitx2*$^{Dermo1\text{-}Cre}$ (B) stained with H&E. Note the absence of cecal bud in the mutant along with a decreased mesenchyme when compared to the control. (C)–(F) BrdU labeling of control (C) and (E) and mutant (D) and (F) cecal sections showed a decreased proliferation in both epithelium and mesenchyme of the mutants. (G) Quantification of the number of BrdU positive cells in the epithelium and the mesenchyme ($n=6$). Scale bars are 50 μm.

conditional knockouts. These results suggest that maintenance of *Fgf10* expression requires mesenchymal *Pitx2*. Conversely, we previously reported that deletion of *Fgf10* in the cecum does not affect the expression of mesenchymal *Pitx2* (Burns et al., 2004). Taken together, these observations indicate that *Fgf10* is downstream of mesenchymal *Pitx2*. In addition, unlike what was observed in the lung (De Langhe et al., 2008), it does not appear that mesenchymal *Pitx2* regulates *Fgfr2c* expression.

Fgf9 regulates Pitx2 expression in the cecum

Specific mesenchymal *Pitx2* inactivation mice show a cecum phenotype similar to the *Fgf9* knockout. However, Fig. 4 shows that epithelial *Fgf9* expression does not depend on mesenchymal *Pitx2* expression. To test whether FGF9 can control *Pitx2* expression, we exposed in vitro cultures of E12.5 cecum for 12 h to 250 ng/mL of recombinant FGF9 in vitro. FGF9-treated ceca showed significant increase in *Pitx2* and *Fgf10* expression, assessed by qRT-PCR, as compared to controls (Fig. 5A), while no changes were observed in the expression of *Fgfr2b or Fgfr2c*. To investigate whether mesenchymal *Fgf9* controls the expression of *Pitx2* in the mesenchyme, we generated mutant embryos with mesenchymal (*Fgf9*$^{Dermo1\text{-}Cre}$) or global (*Fgf9*$^{CMV\text{-}Cre}$) deletion of *Fgf9*, using *Fgf9*$^{f/f}$ mice crossed with *Dermo1-Cre* and *CMV-Cre* respectively. At E14.5, the wild type embryo has a well-developed epithelial cecal bud surrounded by a thick layer of mesenchyme (Fig. 5B). *Fgf9*$^{Dermo1\text{-}Cre}$ embryos with specific inactivation in the mesenchyme displayed a hypoplastic cecum with a narrowed epithelial lumen surrounded by a thinner mesenchyme (Fig. 5C) as compared to the control. By comparison, *Fgf9*$^{CMV\text{-}Cre}$ embryos showed a more severe phenotype with a substantially attenuated epithelial and mesenchymal cecal bud (Fig. 5D). After deletion of mesenchymal *Fgf9*, *Pitx2* was still strongly expressed albeit at a lower level in the *Fgf9*$^{Dermo1\text{-}Cre}$ cecum as compared to control (Fig. 5E and F). Global deletion of *Fgf9* completely abolished the expression of *Pitx2* in the mesenchyme of the *Fgf9*$^{CMV\text{-}Cre}$ gut (Fig. 5G). However, *Pitx2* expression is still detectable in the epithelium at a significant level. In contrast, *Shh* expression was not affected by either mesenchymal or global *Fgf9* deletion (Fig. 5H–J). We conclude that both mesenchymal and epithelial *Fgf9* are important for the formation of the cecum.

Pitx2 induces Fgf10 expression in the absence of Fgf9

To test whether *Pitx2* can directly induce the expression of *Fgf10* in the absence of *Fgf9*, we used an in vitro model of 3T3 cells to overexpress *Pitx2*. We first confirmed the absence of *Fgf9* in these cells by PCR. The transfection of these cells with *Pitx2a* vector resulted in a 7-fold increase of *Pitx2* as assessed by qRT-PCR (data not shown). Moreover, the overexpression of Pitx2 resulted in a significant increase (40%) in the expression of *Fgf10* as compared to the control or the empty vector (Fig. 6). In contrast, no change in *Fgf10* was induced by the empty vector.

Discussion

In humans, the cecum is an important functional part of the GI tract. It is populated by a biodiverse microbiota that play an important role in the digestion of complex carbohydrates delivered from the small intestine (Backhed et al., 2005; Eckburg et al., 2005), and is also a significant site of intestinal immune activity. In the mouse, the cecum develops in 3 phases: bud initiation, bud elongation and bud arrest. To date, the molecular mechanisms regulating these phases are poorly understood. It was recently demonstrated that *Pitx2* null embryos display cecal agenesis (Nichol and Saijoh, 2011). In this report, we show that mesenchymal *Pitx2* regulates both the formation of the cecal mesenchymal bud and the subsequent epithelial bud induction. Absence of mesenchymal *Pitx2* translates into cecal agenesis. However, *Pitx2*$^{Dermo1\text{-}Cre}$ mutants display a less severe phenotype than the Pitx2 null, which was expected. This is due in part to the fact that Pitx2 expression in the epithelium is still maintained. *Pitx2* is mainly implicated in controlling left–right asymmetry during embryonic development (Liu et al., 2001) and is also known to regulate cell proliferation through *cyclinD1* expression in several organs such as the gonads (Rodriguez-Leon et al., 2008). Consistent with previous reports, our data show that cecal agenesis is associated with decreased proliferation in both the epithelium and mesenchyme of the cecum (Burns et al., 2004; Zhang et al., 2006). However, deletion of epithelial *Pitx2* did not adversely affect cecal formation.

Pitx2 has two homologs, *Pitx1* and *Pitx3*. *Pitx1* is expressed in the epithelium and mesenchyme of the developing gut and the cecum (Lanctot et al., 1997; Zacchetti et al., 2007). It is absent in the cecum of mice lacking *HoxD* cluster genes (homeobox domain) that also present with cecal agenesis. *Fgf10* expression

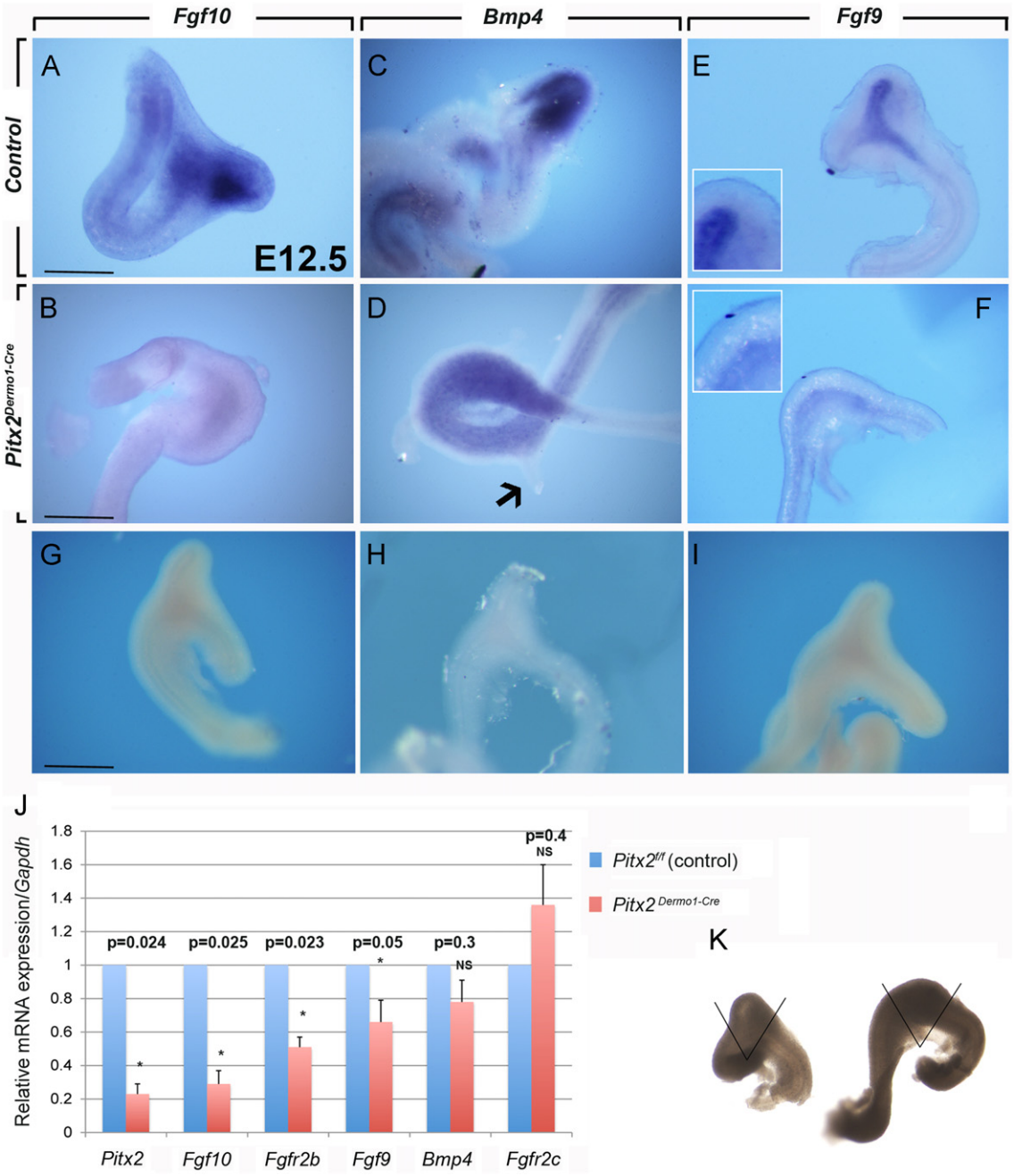

Fig. 4. Gene expression in E12.5 *Pitx2*$^{Dermo1\text{-}Cre}$ cecum. Comparison of *Fgf10*, *Bmp4* (C) and (D) and *Fgf9* (E) and (F) expression by WMISH in ceca isolated at E12.5. *Fgf10* and *Bmp4* are expressed in the mesenchyme of wild type E12.5 cecum ((A) and (C) respectively). *Fgf10* expression is absent from the cecum of the mutants (B) while *Bmp4* expression is maintained in the mutant ceca (D). *Fgf9* is expressed in both epithelium and mesenchyme of E12.5 WT cecum (E) and its expression is restricted to the epithelium of the mutant ceca (F). Insets in (E) and (F) show a high magnification of the cecal bud. (G)–(I) Negative controls using the sense probes for *Fgf10* (G), *Bmp4* (H) and *Fgf9* (I) did not show any staining. (J) Quantification of gene expression by RT-qPCR ($n=12$). (K) Schematic illustration of the parts of the ceca from controls and mutants that were used for the analyses. Scale bars are 500 μm.

is also drastically reduced in these mice (Zacchetti et al., 2007), suggesting a role for *Pitx1* in cecal formation as well as *Fgf10* expression. However, *Pitx1* null embryos display normal cecum formation (Supplementary Fig. S1). *Pitx3* is mainly expressed in skeletal muscle, eye, midbrain and forebrain as demonstrated by WISH and *Pitx3–GFP* or *Pitx3–LacZ* reporter mice (Coulon et al., 2007; Grealish et al., 2010; L'Honore et al., 2007; Zhao et al., 2004). *Pitx3* expression in developing gut or cecum has not been reported. This indicates a unique role for mesenchymal *Pitx2* in coordinating cecal formation. However, we cannot exclude a possible functional redundancy between *Pitx1* and *Pitx2* in the epithelium.

An FGF9–Pitx2–FGF10 signaling pathway controls cecal formation

We have previously shown that, in lung development, *Pitx2* positively regulates *Fgfr2c* transcription. Through this mechanism, Pitx2 directly impacts the ability of the mesenchyme to respond to FGF9 and thus to maintain *Fgf10* expression (De Langhe et al., 2008). Moreover, Fgf10 is strongly expressed in the mesenchyme of the cecum (El Agha et al., 2012). These results led us to propose that an FGF9/Pitx2/FGF10 signaling pathway could control bud formation. Our current results demonstrate that this model applies, at least partially, to the cecum as we found that epithelial FGF9 controls mesenchymal *Pitx2* expression, which in turn

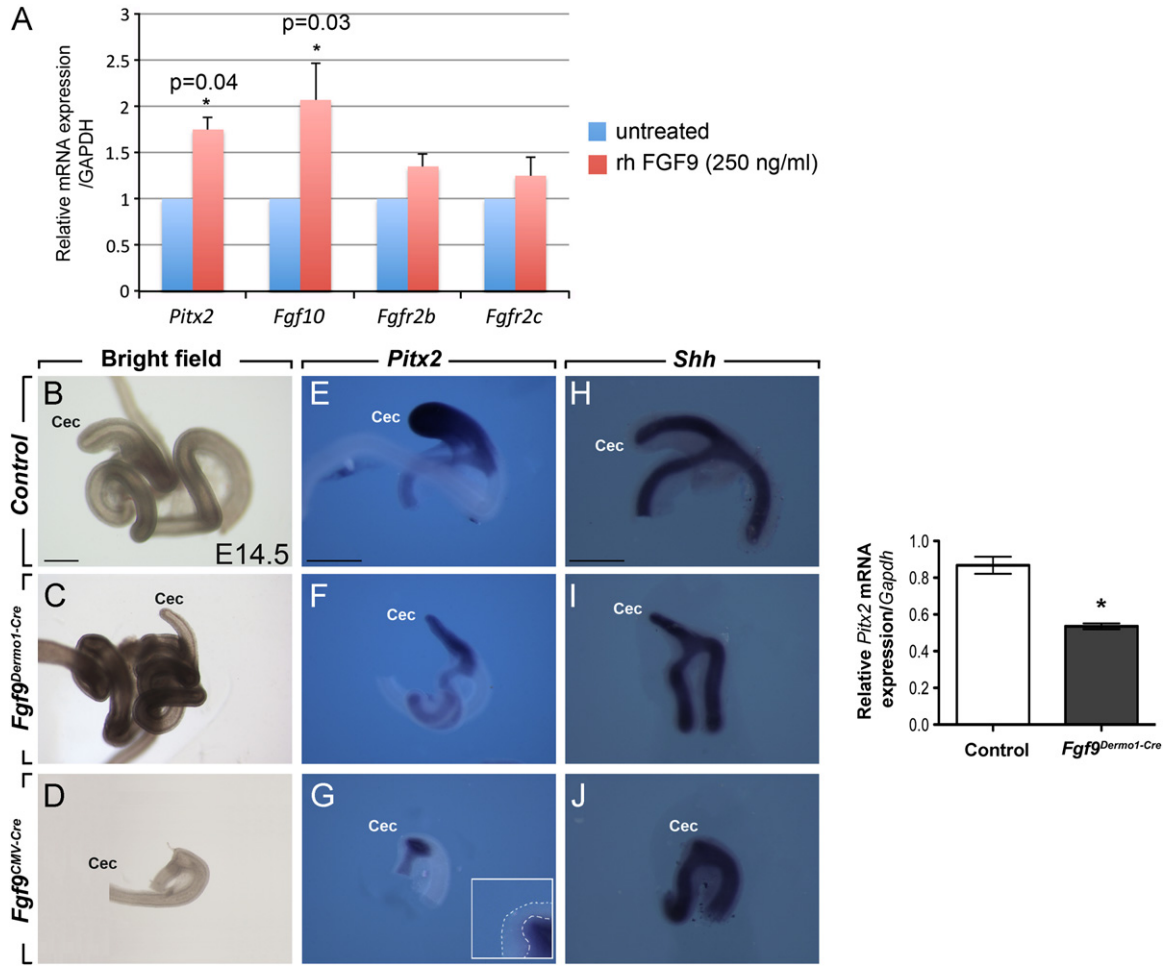

Fig. 5. FGF9 controls the expression of *Pitx2* and *Fgf10*. (A) qPCR for *Pitx2*, *Fgf10*, *Fgfr2b and Fgfr2c* after in vitro culture of ceca in the absence or presence of 250 ng/mL rh FGF9 for 12 h ($n=4$ in duplicates). (B)–(D) Comparison of the cecum development at E14.5 in wild type (B), $Fgf9^{Dermo1\text{-}Cre}$ (C) and $Fgf9^{CMV\text{-}Cre}$ (D) mutants. The wild type cecum has a well developed cecal bud surrounded by a thick layer of mesenchyme (B); deletion of *Fgf9* in the mesenchyme resulted in a thinning of the mesenchymal layer surrounding the epithelial bud that forms properly (C), whereas the complete deletion of *Fgf9* resulted in impaired cecal bud formation (D). *Pitx2* (E)–(G) and *Shh* (H)–(J) expression in mutants compared to the control. Note the complete lack of *Pitx2* expression in the mesenchyme of $Fgf9^{CMV\text{-}Cre}$ gut ((G) inset shows a high magnification of the cecal bud). No detectable change in *Shh* expression was detected in either mutants (I) and (J) compared to control (H). Scale bars are 250 μm.

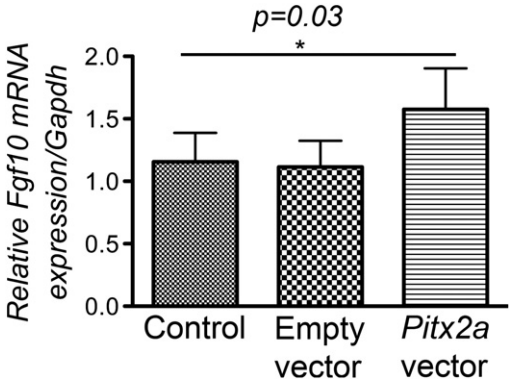

Fig. 6. Pitx2 overexpression induced the expression of *Fgf10* in the absence of *Fgf9*. Relative *Fgf10* mRNA expression showed significant increase of *Fgf10* expression after transfection of NIH 3T3 cells (negative for *Fgf9*) with *Pitx2a* vector ($n=4$, $p=0.03$).

controls mesenchymal *Fgf10* expression. However, *Fgfr2c* expression was not changed upon mesenchymal *Pitx2* inactivation, suggesting that *Pitx2* does not control *Fgfr2c* or that other compensatory pathways could be involved. Further studies will be needed to characterize the regulators of *Fgfr2c* expression in the cecal mesenchyme.

Fibroblast Growth factors 9 and 10 along with their cognate receptors FGFR2c and FGFR2b, respectively, are known regulators of cecal development. *Fgf9* is essential for mesenchymal cecal bud induction and controls *Fgf10* expression. In turn, the FGF10/FGFR2b pathway is critical for the subsequent elongation phase of the epithelial cecal bud into the newly formed cecal mesenchyme (Burns et al., 2004; Fairbanks et al., 2004; Zhang et al., 2006). FGF10, from the mesenchyme, signals to the epithelium via its receptor FGFR2b. The FGF10/FGFR2b pathway is known to induce epithelial branching in several organ systems including lung, salivary glands and mammary glands (Min et al., 1998; Parsa et al., 2008; Sekine et al., 1999; Steinberg et al., 2005). Both *Fgf10* and *Fgfr2b* null mice fail to develop a cecal epithelial bud (Burns et al., 2004) but still exhibit a significant mesenchymal bud while *Fgf9* null embryos exhibited a complete absence of the epithelial and mesenchymal cecal bud. In this report we show that, similar to total *Fgf9* knockout, deletion of *Pitx2* in the mesenchyme results in the complete absence of mesenchymal cecal bud formation. Moreover, we showed that *Pitx2* induces the expression of *Fgf10* in the absence of *Fgf9*, therefore positioning *Pitx2* downstream of *Fgf9*. These observations, along with the in vitro cecal cultures in the presence of recombinant FGF9, confirm our

hypothesis that FGF9 acts upstream of *Pitx2* during cecal development. In addition, the decrease of *Fgf10* and *Fgfr2b* expression in *Pitx2*$^{Dermo1\text{-}Cre}$ mutants is consistent with what was observed in the *Fgf9* null mutants.

Epithelial but not mesenchymal Fgf9 is required for cecal budding

It has been proposed that epithelial but not mesenchymal *Fgf9* is required for cecal budding and elongation (Zhang et al., 2006). Our results demonstrate that mesenchymal *Fgf9* is also an important player in the elongation of the cecal bud as mesenchymal *Fgf9* deletion resulted in the formation of a shorter cecum and a thinner mesenchyme, accompanied with a decrease in *Pitx2* expression. However, global *Fgf9* deletion resulted in a much more severe phenotype, displaying only an attempt to form a rudimentary epithelial bud and a complete absence of mesenchymal *Pitx2* expression. This rudimentary bud formation upon complete *Fgf9* deletion could be due to variable or partial penetrance of the previously described *Fgf9* null phenotype. However, as implied by global *Fgf9* inactivation, epithelial *Fgf9* is likely the key player in the initial steps of cecal formation.

An FGF9–Pitx2 axis controls the elongation of the small intestine

Fgf10 expression is restricted to the caudal cecal mesenchyme while *Fgf9* is expressed in both the epithelium and the mesenchyme of the developing small intestine, cecum and colon (Zhang et al., 2006). Interestingly, in the small intestine *Pitx2* expression is restricted to the epithelium during early stages of development (E11.5–E12.5) and then starts to be expressed in the mesenchyme around E13.5. Our data indicate that mesenchymal *Pitx2* expression is critical for the proper extension of the small intestine during development. *Fgf9* null mutants showed a decrease in the length of the small intestine (about 80% of the control length at E14.5) (Zhang et al., 2006) similar to that observed for *Pitx2*$^{Dermo1\text{-}Cre}$ mutants. In both mutants (*Fgf9* and *Pitx2*), this difference is noticeable mostly from E14.5 onwards, a time-point when *Pitx2* is expressed in the mesenchyme. Taken together, these findings suggest that *Pitx2* function downstream of *Fgf9* is important for the elongation of the small intestine. This possibility is supported by the fact that the development of the colon, where *Fgf9* is expressed but not *Pitx2*, is not affected by the deletion of *Fgf9* (Geske et al., 2008). We therefore speculate an important role for *Pitx2* in controlling the elongation of the small intestine. Further analyses to test that hypothesis could be carried out. For example, expressing *Pitx2* in the colon mesenchyme (where it is normally absent) could help determine whether or not this is sufficient to trigger excessive elongation.

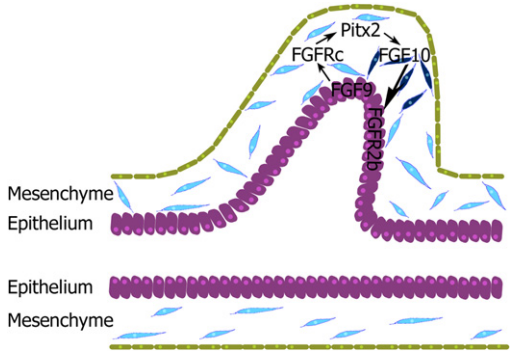

Fig. 7. Model of FGF/Pitx2/FGF10 signaling in the developing cecum. We propose that epithelial FGF9 acts via FGFRc receptor isoforms in the mesenchyme to control cecal mesenchyme expansion and *Fgf10* expression. Both activities are mediated by Pitx2. In turn FGF10 acts on the epithelium to trigger the invasion of the epithelial bud into the cecal mesenchyme.

In conclusion, *Fgf9* compartment-specific deletions suggest that both epithelial and mesenchymal FGF9 are important for the proper formation of the cecum and that both sources control mesenchymal *Pitx2* expression. In addition, the phenotype of *Pitx2*$^{Dermo1\text{-}Cre}$ mice suggests that FGF9 controls mesenchymal proliferation and acts mainly through mesenchymal Pitx2 to induce *Fgf10* expression. In turn, FGF10 controls cecal epithelial budding and elongation (Fig. 7).

Acknowledgments

D.A.A. acknowledges previous support of the American Lung Association and current support from the American Heart Association. S.B. acknowledges support from the NIH (nos. HL086322, HD052609 and HL074832) and the Excellence Cluster in Cardio-Pulmonary system, Giessen, Germany. M.R.F. is supported by the NIH awards nos. DK077956 and DK090295. Tracy Grikscheit acknowledges support from the California Institute for Regenerative Medicine (CIRM) (no. RN2009461). We would like to thank Jonathan Branch for the maintenance of the different mouse colonies needed for this project and Clarence Wigfall for critical reading of the manuscript.

Appendix A. Supporting information

Supplementary data associated with this article can be found in the online version at http://dx.doi.org/10.1016/j.ydbio.2012.07.008.

References

Arakawa, H., Nakamura, T., Zhadanov, A.B., Fidanza, V., Yano, T., Bullrich, F., Shimizu, M., Blechman, J., Mazo, A., Canaani, E., Croce, C.M., 1998. Identification and characterization of the ARP1 gene, a target for the human acute leukemia ALL1 gene. Proc. Nat. Acad. Sci. U. S. A. 95, 4573–4578.

Backhed, F., Ley, R.E., Sonnenburg, J.L., Peterson, D.A., Gordon, J.I., 2005. Host-bacterial mutualism in the human intestine. Science 307, 1915–1920.

Bellusci, S., Grindley, J., Emoto, H., Itoh, N., Hogan, B.L., 1997. Fibroblast growth factor 10 (FGF10) and branching morphogenesis in the embryonic mouse lung. Development 124, 4867–4878.

Burns, R.C., Fairbanks, T.J., Sala, F., De Langhe, S., Mailleux, A., Thiery, J.P., Dickson, C., Itoh, N., Warburton, D., Anderson, K.D., Bellusci, S., 2004. Requirement for fibroblast growth factor 10 or fibroblast growth factor receptor 2-IIIb signaling for cecal development in mouse. Dev. Biol. 265, 61–74.

Campione, M., Steinbeisser, H., Schweickert, A., Deissler, K., van Bebber, F., Lowe, L.A., Nowotschin, S., Viebahn, C., Haffter, P., Kuehn, M.R., Blum, M., 1999. The homeobox gene Pitx2: mediator of asymmetric left-right signaling in vertebrate heart and gut looping. Development 126, 1225–1234.

Cardoso, W.V., 2001. Molecular regulation of lung development. Annu. Rev. Physiol. 63, 471–494.

Coulon, V., L'Honore, A., Ouimette, J.F., Dumontier, E., van den Munckhof, P., Drouin, J., 2007. A muscle-specific promoter directs Pitx3 gene expression in skeletal muscle cells. J. Biol. Chem. 282, 33192–33200.

De Langhe, S.P., Carraro, G., Tefft, D., Li, C., Xu, X., Chai, Y., Minoo, P., Hajihosseini, M.K., Drouin, J., Kaartinen, V., Bellusci, S., 2008. Formation and differentiation of multiple mesenchymal lineages during lung development is regulated by beta-catenin signaling. PLoS One 3, e1516.

Eckburg, P.B., Bik, E.M., Bernstein, C.N., Purdom, E., Dethlefsen, L., Sargent, M., Gill, S.R., Nelson, K.E., Relman, D.A., 2005. Diversity of the human intestinal microbial flora. Science 308, 1635–1638.

El Agha, E., Al Alam, D., Carraro, G., Mackenzie, B., Goth, K., De Langhe, S., Voswinckel, R., Hajihosseini, M.K., Rehan, V.K., Bellusci, S., 2012. Characterization of a novel fibroblast growth factor 10 (Fgf10) knock-in mouse line to target mesenchymal progenitors during embryonic lung development. PLoS One 7 (6), e38452.

Fairbanks, T.J., Kanard, R.C., De Langhe, S.P., Sala, F.G., Del Moral, P.M., Warburton, D., Anderson, K.D., Bellusci, S., Burns, R.C., 2004. A genetic mechanism for cecal atresia: the role of the Fgf10 signaling pathway. J. Surg. Res. 120, 201–209.

Gage, P.J., Camper, S.A., 1997. Pituitary homeobox 2, a novel member of the bicoid-related family of homeobox genes, is a potential regulator of anterior structure formation. Hum. Mol. Genet. 6, 457–464.

Gage, P.J., Suh, H., Camper, S.A., 1999. Dosage requirement of Pitx2 for development of multiple organs. Development 126, 4643–4651.
Geske, M.J., Zhang, X., Patel, K.K., Ornitz, D.M., Stappenbeck, T.S., 2008. Fgf9 signaling regulates small intestinal elongation and mesenchymal development. Development 135, 2959–2968.
Grealish, S., Jonsson, M.E., Li, M., Kirik, D., Bjorklund, A., Thompson, L.H., 2010. The A9 dopamine neuron component in grafts of ventral mesencephalon is an important determinant for recovery of motor function in a rat model of Parkinson's disease. Brain 133, 482–495.
Green, P.D., Hjalt, T.A., Kirk, D.E., Sutherland, L.B., Thomas, B.L., Sharpe, P.T., Snead, M.L., Murray, J.C., Russo, A.F., Amendt, B.A., 2001. Antagonistic regulation of Dlx2 expression by PITX2 and Msx2: implications for tooth development. Gene Expression 9, 265–281.
Hjalt, T.A., Semina, E.V., Amendt, B.A., Murray, J.C., 2000. The Pitx2 protein in mouse development. Dev. Dyn. 218, 195–200.
Kitamura, K., Miura, H., Yanazawa, M., Miyashita, T., Kato, K., 1997. Expression patterns of Brx1 (Rieg gene), Sonic hedgehog, Nkx2.2, Dlx1 and Arx during zona limitans intrathalamica and embryonic ventral lateral geniculate nuclear formation. Mech. Dev. 67, 83–96.
Koike, T., Yasugi, S., 1999. In vitro analysis of mesenchymal influences on the differentiation of stomach epithelial cells of the chicken embryo. Differentiation 65, 13–25.
Kozlowski, K., Walter, M.A., 2000. Variation in residual PITX2 activity underlies the phenotypic spectrum of anterior segment developmental disorders. Hum. Mol. Genet. 9 (14), 2131–2139.
L'Honore, A., Coulon, V., Marcil, A., Lebel, M., Lafrance-Vanasse, J., Gage, P., Camper, S., Drouin, J., 2007. Sequential expression and redundancy of Pitx2 and Pitx3 genes during muscle development. Dev. Biol. 307, 421–433.
Lanctot, C., Lamolet, B., Drouin, J., 1997. The bicoid-related homeoprotein Ptx1 defines the most anterior domain of the embryo and differentiates posterior from anterior lateral mesoderm. Development 124, 2807–2817.
Lin, Y., Liu, G., Wang, F., 2006. Generation of an Fgf9 conditional null allele. Genesis 44, 150–154.
Liu, C., Liu, W., Lu, M.F., Brown, N.A., Martin, J.F., 2001. Regulation of left-right asymmetry by thresholds of Pitx2c activity. Development 128, 2039–2048.
Min, H., Danilenko, D.M., Scully, S.A., Bolon, B., Ring, B.D., Tarpley, J.E., DeRose, M., Simonet, W.S., 1998. Fgf-10 is required for both limb and lung development and exhibits striking functional similarity to Drosophila branchless. Genes Dev. 12, 3156–3161.
Muccielli, M.L., Martinez, S., Pattyn, A., Goridis, C., Brunet, J.F., 1996. Otlx2, an Otx-related homeobox gene expressed in the pituitary gland and in a restricted pattern in the forebrain. Mol. Cell. Neurosci. 8, 258–271.
Nichol, P.F., Saijoh, Y., 2011. Pitx2 is a critical early regulatory gene in normal cecal development. J. Surg. Res. 170 (1), 107-111.
Parsa, S., Ramasamy, S.K., De Langhe, S., Gupte, V.V., Haigh, J.J., Medina, D., Bellusci, S., 2008. Terminal end bud maintenance in mammary gland is dependent upon FGFR2b signaling. Dev. Biol. 317, 121–131.
Rodriguez-Leon, J., Rodriguez Esteban, C., Marti, M., Santiago-Josefat, B., Dubova, I., Rubiralta, X., Izpisua Belmonte, J.C., 2008. Pitx2 regulates gonad morphogenesis. Proc. Nat. Acad. Sci. U. S. A. 105, 11242–11247.
Sekine, K., Ohuchi, H., Fujiwara, M., Yamasaki, M., Yoshizawa, T., Sato, T., Yagishita, N., Matsui, D., Koga, Y., Itoh, N., Kato, S., 1999. Fgf10 is essential for limb and lung formation. Nat. Genet. 21, 138–141.
Semina, E.V., Datson, N.A., Leysens, N.J., Zabel, B.U., Carey, J.C., Bell, G.I., Bitoun, P., Lindgren, C., Stevenson, T., Frants, R.R., van Ommen, G., Murray, J.C., 1996a. Exclusion of epidermal growth factor and high-resolution physical mapping across the Rieger syndrome locus. Am. J. Hum. Genet. 59, 1288–1296.
Semina, E.V., Reiter, R., Leysens, N.J., Alward, W.L., Small, K.W., Datson, N.A., Siegel-Bartelt, J., Bierke-Nelson, D., Bitoun, P., Zabel, B.U., Carey, J.C., Murray, J.C., 1996b. Cloning and characterization of a novel bicoid-related homeobox transcription factor gene, RIEG, involved in Rieger syndrome. Nat. Genet. 14, 392–399.
Shannon, J.M., Hyatt, B.A., 2004. Epithelial–mesenchymal interactions in the developing lung. Annu. Rev. Physiol. 66, 625–645.
Steinberg, Z., Myers, C., Heim, V.M., Lathrop, C.A., Rebustini, I.T., Stewart, J.S., Larsen, M., Hoffman, M.P., 2005. FGFR2b signaling regulates ex vivo submandibular gland epithelial cell proliferation and branching morphogenesis. Development 132, 1223–1234.
Winnier, G., Blessing, M., Labosky, P.A., Hogan, B.L., 1995. Bone morphogenetic protein-4 is required for mesoderm formation and patterning in the mouse. Genes Dev. 9, 2105–2116.
Yu, K., Xu, J., Liu, Z., Sosic, D., Shao, J., Olson, E.N., Towler, D.A., Ornitz, D.M., 2003. Conditional inactivation of FGF receptor 2 reveals an essential role for FGF signaling in the regulation of osteoblast function and bone growth. Development 130, 3063–3074.
Zacchetti, G., Duboule, D., Zakany, J., 2007. Hox gene function in vertebrate gut morphogenesis: the case of the caecum. Development 134, 3967–3973.
Zhang, X., Stappenbeck, T.S., White, A.C., Lavine, K.J., Gordon, J.I., Ornitz, D.M., 2006. Reciprocal epithelial–mesenchymal FGF signaling is required for cecal development. Development 133, 173–180.
Zhao, S., Maxwell, S., Jimenez-Beristain, A., Vives, J., Kuehner, E., Zhao, J., O'Brien, C., de Felipe, C., Semina, E., Li, M., 2004. Generation of embryonic stem cells and transgenic mice expressing green fluorescence protein in midbrain dopaminergic neurons. Eur. J. Neurosci. 19, 1133–1140.